Available online at www.sciencedirect.com

ScienceDirect

Procedia Engineering 86 (2014) 767 – 774

Procedia Engineering

www.elsevier.com/locate/procedia

1st International Conference on Structural Integrity, ICONS-2014

Modeling, Prediction and Validation of Thermal Cycles, Residual Stresses and Distortion in type 316 LN Stainless Steel Weld Joint made by TIG Welding Process

K.C. Ganesh[a], M. Vasudevan[b,*], K.R. Balasubramanian[a], N. Chandrasekhar[b], S. Mahadevan[b], P. Vasantharaja[b] and T. Jayakumar[b]

[a]*Department of Mechanical Engineering, National Institute of Technology, Tiruchirappalli - 620015, India.*
[b]*Metallurgy and Materials Group, Indira Gandhi Centre for Atomic Research, Kalpakkam - 603102, India.*
[*]*E-mail ID: dev@igcar.gov.in*

Abstract

In this research work, Finite Element Modeling (FEM) using SYSWELD was carried out to predict thermal cycles, residual stresses and distortion in type 316 LN stainless steel weld joint made by TIG welding process. The numerically predicted thermal cycles and temperature distribution were validated using Infrared (IR) Thermography. The model predictions of the surface and bulk residual stress profiles were validated using X-ray Diffraction (XRD) and Ultrasonic Testing (UT) respectively. Distortion analysis was also performed and validated using digital height gauge measurement. IR thermography was found to be a good tool for validating the model predictions of the temperature distribution in the weld joint. There was good agreement between the model predictions and the experimentally observed values of temperature, residual stresses and distortion. Therefore, the numerical modeling in combination with non-destructive methods provides an efficient approach for predicting the effect of welding process on the weld attributes.

Peer-review under responsibility of the Indira Gandhi Centre for Atomic Research

Keywords: FEM, TIG Welding, Thermal Cycles, Residual Stresses, Distortion, Infrared Thermography.

1. Introduction

In the fusion welding process due to localized heating and cooling, residual stresses and distortion occur near the welded region. Also, the high temperature developed in the welded zone significantly changes the metallurgical properties of the joint. Therefore, accurate prediction of thermal cycles, residual stress and distortion in the weld joint during welding is essential for controlling the evolution of microstructure, residual stresses and distortion for the given heat input. Many investigators developed numerical models to study the effect of welding

Peer-review under responsibility of the Indira Gandhi Centre for Atomic Research
doi:10.1016/j.proeng.2014.11.096

process parameters on the above mentioned weld attributes.

In the recent paper, Joy Varghese et al. [1] reviewed the recent trends in the heat transfer analysis during TIG welding and emphasized the non-availability of procedure to couple the multi physics of welding. De and Debroy [2] reviewed extensively on modeling of welding residual stresses and mentioned the challenges in residual stress prediction using 3D finite element model and experiments. Eagar and Tsai [3] proposed an analytical method for predicting temperature fields produced by a moving distributed heat source. Further Tsai and Eagar [4] mentioned that the weld process parameters and material properties were significant in the weld pool shape prediction.

Goldak et al.[5] proposed the description of arc heat source which was named as 'double ellipsoidal' heat source. They suggested that appropriate parameters of heat source could be arrived by direct measurement of a weld experiment. Goldak et al. [6] further discussed about the need of heat transfer model as it was the driving force for the stress and microstructure analysis. Nguyen et al. [7] derived an analytical solution for thermal field from a 3D double ellipsoidal power density heat source. Zhu and Chao [8] discussed that specific material properties especially thermal conductivity and yield stress were sensitive to the process and other properties could be considered in the room temperature. Asserin et al.[9] made very detailed systematic sensitivity analysis to predict the important material properties for the simulation. Barroso et al. [10] used simplified material model to reduce the solver time and performed semi destructive stress measurements for the prediction of residual stresses.

Aarbogh et al. [11] performed numerical distortion analysis on austenitic stainless steels. The heat source calibration was not based on experiment and explained the inaccuracy of using thermocouple measurement. Attarha and Far [12] analysed similar and dissimilar plate welding by numerical modeling and validated experimentally using thermocouples. They suggested that the measurements using thermocouples should be cautious, as it would not give accurate measurements if any junctions present along the thermocouple. It was found that very limited research work has been performed in AISI 316LN stainless steel. Also, limited work has been carried out using Infrared thermography to validate the model predictions using FEM. Bulk residual stress measurements and the model predictions were not correlated well. This work addresses the above mentioned gap. The distortion prediction was validated using digital height gauge and the nominal residual stress was validated by ultrasonic testing. The predictions were noticeably agreed with the experimental validations.

2. Experimental Procedure

2.1. TIG Welding

In the nuclear industry, reactor vessels, vessel liners, pressure channels, fuel claddings, heat exchangers, condenser tubes, pipes etc., are fabricated using AISI 316LN grade austenitic stainless steels. In this investigation, TIG welding of 316LN steel plates was performed with the dimensions given in Figure.1. The butt joint was made using automated TIG welding machine with 100mm/min welding speed, 100A current, 3mm arc gap and 10 lt/hr flow rate of argon shielding gas. In the experimental setup, the IR camera was mounted behind the welding torch. It captures the molten pool image and stored in a personal computer.

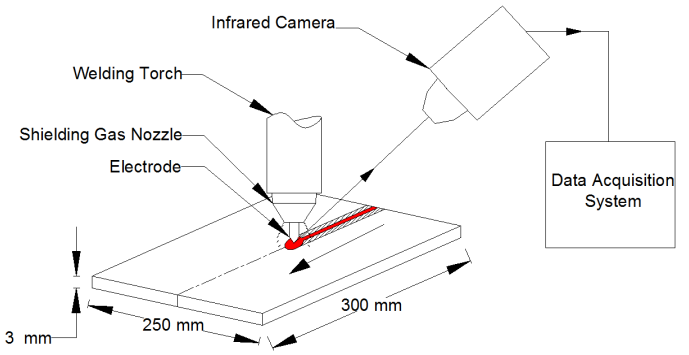

Fig.1. Schematic Sketch of Gas tungsten arc welding process with an IR camera

2.2. IR Thermography

IR Thermography is one of the promising NDE technologies to analyse the induced isotherms in welding [13]. It does not emit radiation whereas it records the emitted radiation from the material. The amount of radiation depends on the material's temperature.

2.3. Distortion Measurement

The distortion of steel plates was measured using digital height gauge at different locations. The out of plane distortions were measured at 25mm x 20mm size grids mapped on the plates. The steel plates were placed on the granite surface plate and the digital height gauge was moved to its each grid point to measure the distortion before and after the welding process.

2.4. Residual Stress Measurement

Ultrasonic testing (UT) was used to measure the residual stress which is based on the effects of stress on the propagation of elastic waves. The critically refracted longitudinal (L_{CR}) waves are sensitive to the residual stresses induced in the components. In this research work, a 2MHz probe was used to generate L_{CR} waves to penetrate 3mm plate by fixing the probe at a first critical angle of 28°. The critical angle can be calculated using Snell's law,

$$[(\sin \theta_{Pr}) / (C_{Pr})] = [(\sin \theta_s) / (C_s)] \quad (1)$$

Where, θ_{Pr} is the angle of the incident wave in the Perspex and θ_S is the angle of refracted wave in the steel. C_{Pr} is the wave speed in the Perspex (2730m/s) and C_S is the wave speed in steel (5900m/s). Based on the acousto-elasticity theory, the acoustic elastic constant (AEC) for a given material is defined in terms of transit time and is given in the equation (2),

$$B = (t - t_0) / \sigma \quad (2)$$

Where, t is the measured ultrasonic transit time, t_0 is the transit time measured with zero load condition. B is the AEC and σ is the applied or residual stress. The AEC was calculated as 0.588ns MPa^{-1} for the AISI 316LN material using the UT probe assembly developed in Indira Gandhi Centre for Atomic Research (IGCAR), India [14]. In the weld joint the magnitude of the longitudinal stress component is much higher than the transverse stress component and in equation (2), σ is considered as a uniaxial stress component.

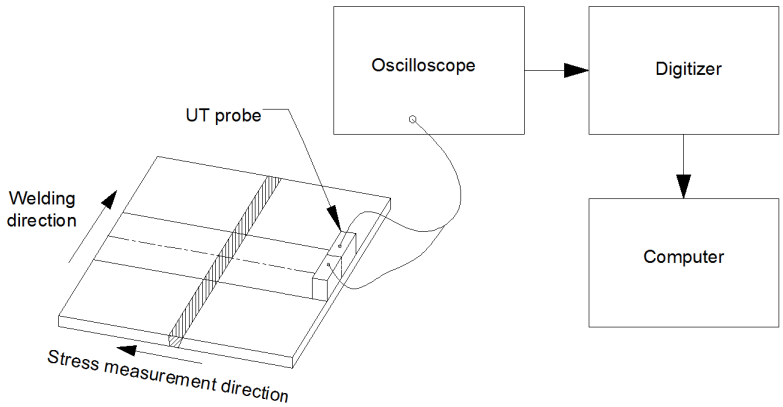

Fig.2. Ultrasonic Testing Setup

Figure.2 shows the schematic representation of UT setup. The data acquisition system collects the transit time of the wave propagation from the probe which can be monitored with an oscilloscope and stored in a computer using a digitizer.

3. Numerical Modeling

The finite element analysis of welding simulation was performed by sequentially coupled formulation. The molten pool was modeled using double ellipsoidal volumetric heat source.

3.1. Governing Equations

The heat is dispersed from the weld zone, primarily through conduction into the surrounding material of the work piece. The conduction depends on the thermal properties of the metal, weld bead geometry and the ambient temperature (preheat) of the metal. Heat conduction can be described by solving the heat equation.

$$\nabla (k \nabla T) + Q(x, y, z, t) = \rho C_p (\partial T / \partial t) \quad (4)$$

Where, Q = source rate of heat in domain (W m^{-3}), ρ = Density (kg m^{-3}), k = Thermal conductivity (W m^{-1} °C^{-1}), C_p = Specific heat (J kg^{-1} °C^{-1}), T = Transient temperature (°C), t = time (s). The convective and radiative heat losses during welding is governed by Newton's law of cooling and Stefan-Boltzmann relation are given as follow,

$$q_c = h (T_w - T_a) \quad (5)$$

$$q_r = \sigma \varepsilon (T_w^4 - T_a^4) \quad (6)$$

Where, q_c, q_r = Heat flux during convective and radiative losses respectively (W m^{-2}), T_w, T_a = Surface and surrounding temperature respectively (°C), h = Heat transfer coefficient for convection (W m^{-2} °C^{-1}), σ = Stefan-Boltzmann constant (W m^{-2} °C^{-4}), ε = Emissivity. In the thermo-mechanical analysis, the thermal history was applied to predict the mechanical behavior. The plastic deformation of materials assumed to obey the von-Mises yield criteria.

3.2. Material Modeling

Material modeling is one of the challenging tasks in the welding simulation. The required material properties of AISI 316LN were obtained from IGCAR data book [15]. The convection stirring in the molten pool was balanced in the present analysis by artificially increasing the thermal conductivity of the material after melting point. These assumptions have significant influence in the thermal modeling.

3.3. Finite Element Model

A symmetry model was used for the FEM analysis, but it is mirrored in the figure 3 for better understanding. In the welding zone up to 20mm, the mesh was refined. The model was generated with $1.9*10^5$ 3D solid elements. The model was created such that the welding path was parallel to the Y axis and it was placed on the XY plane.

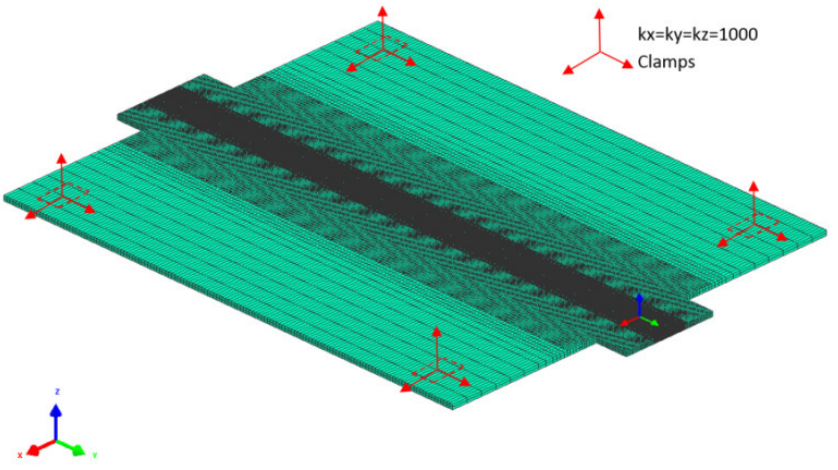

Fig.3. FE Model

3.4. Initial and Boundary Conditions

The experiment was performed in a temperature controlled environment. The initial condition was taken as 20°C. The YZ plane was assigned as symmetry plane. The model was assumed convective and radiative losses on its surfaces except the symmetry plane. The convective losses were taken as 25W m^{-2}. A force free clamping was provided as shown in the Figure 3.

4. Results and Discussion

4.1. Temperature Distribution

Figure 4 is plotted for nodes up to 20 mm from the center line in the transverse direction of welding. It shows the induced peak temperature which keeps on reducing in transverse direction. It is evident that the temperature away from the weld zone is less which does not get influenced more by the welding process. The direct impact of heat input on the surface induces higher heat on surface whereas the bottom temperature reduces due to the heat transfer. The temperature rate in the welding process is different depending on the time during welding. The maximum heating and cooling rate are taken in the quasi-steady state condition.

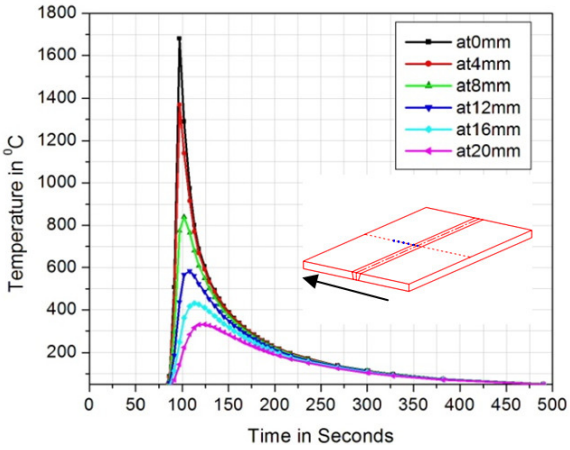

Fig.4. Thermal cycle in transverse direction

Based on the infrared thermography and FE analysis, the thermal heat source profiles were obtained as shown in Figure.5. In the quasi steady state condition the thermal profiles match with each other. The profiles observed by the experiment and by numerical model is found to be in good agreement. The peak temperature observed in both the methods are in good agreement in quasi-steady state condition. The peak temperature matches with experimental work. The small deviation observed in the comparison is due to the material modeling assumptions made above the melting point. Also the experimental limitations in reality contribute to the small variations. These variations further can be reduced by improving the FEM analysis by considering proper weld pool convection effects and boundary conditions in the model.

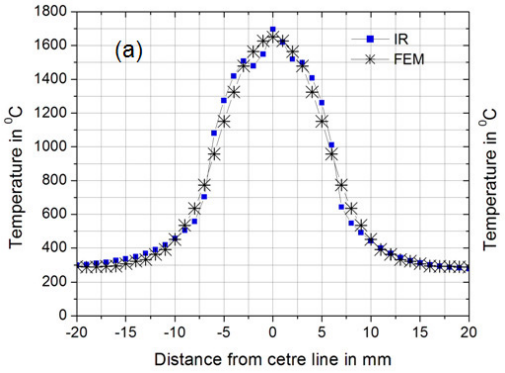

Fig.5. Temperature in FEM and IR comparison at 50s

4.2. Residual Stress Analysis

The residual stress measurement was performed using XRD and UT. Numerical predictions of the residual stress profiles were validated by longitudinal residual stress measurements taken at the center of plates. In XRD the surface residual stress was measured which also validated using FEA as given in Figure.6.(a). In the UT measurement, the waves would penetrate up to 3mm so that it could not be compared directly. Residual stress values from the UT are compared with the average stress values interpreted from the model. Figure 6.(b) shows that UT experimental stress measurements noticeably agreed with the numerical prediction.

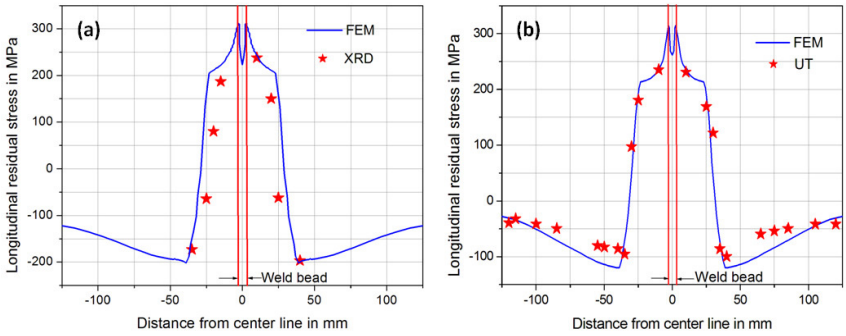

Fig.6. Residual stress comparison (A). FEM vs XRD, (b). FEM vs UT

The higher stress concentration at heat affected zone occurs due to the balance between solidification of molten pool and shrinkage resistance of base material. Away from the heat affected zone the tensile stress gradually transfers into compressive stress. In both experiments, measured peak residual stress at 15 mm away from the center line reaches up to 230 MPa. Towards the edge of plates the nominal stress components remains compressive.

4.3. Distortion Analysis

In general, welding involves the thermal distribution and corresponding plastic deformation. Thinner plates are used for the fabrication when high strength materials and its alloys are employed. In this case, the welding process induces buckling mode of deformation. It could be predicted by implementing the large deformation theory where geometrical nonlinearity also taken into account in the prediction of deformation.

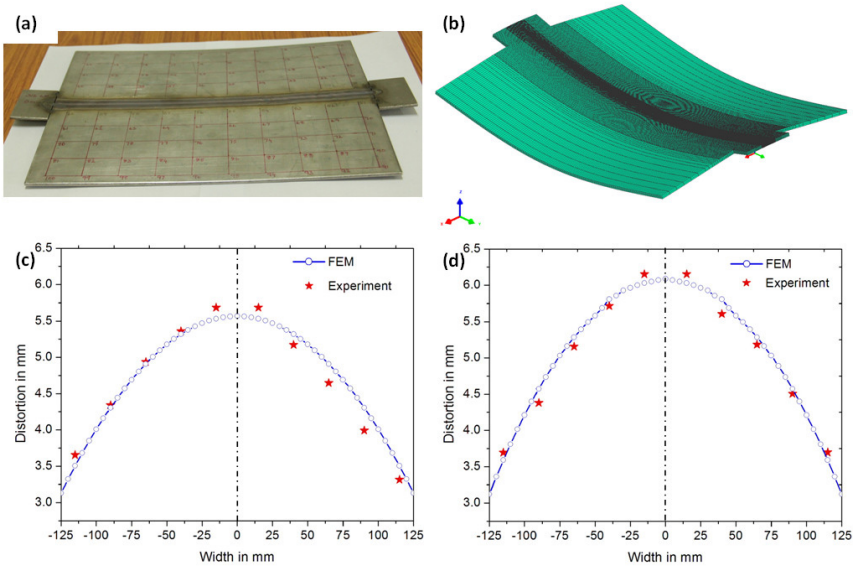

Fig.7. Distortion comparison, (a).After welding experiment, (b).After welding FEM (magnified 5x), (c).Left edge transverse distortion, (d). Right edge transverse distortion

The Figure.7.(a and b) shows the distorted plate and corresponding FE model after welding. The welded plates were distorted (bowed) once the clamps were released. This distortion is due to the release of induced residual stresses during welding. Longitudinal shrinkage was restricted by the tack weld, run-in and run-out plates and also the clamps provided at the plate corner lead to buckling distortion. The predicted distortion at the left and right side transverse edge agree well with the experimental measurements as shown in Figure.7.(c and d). It is obvious from the Figure.7.(c and d) that the heat accumulation during welding induces higher distortion at the right side edge.

5. Conclusions

In this study, a systematic procedure was followed to perform the thermo-mechanical TIG welding analysis using FEM and it was validated by experiments. Based on the research work, the conclusions are summarized as follows:

- In the numerical model the proper calibration of heat source based on experimental measurements were incorporated such that final temperature distribution were correlated with the experimental measurements which overcomes the uncertainty of results.
- The temperatures were observed using IR and FEA which ensures that the process has negligible temperature change at the quasi-steady state condition. It reaches up to 1686°C. There is good agreement between the predicted and measured thermal cycles.
- Infra red thermogrpahy was found to be good tool for validating the thermal cycle predictions by FEM.
- The residual stress predictions agree with experimental measurement which has reasonable accuracy. It ensures that the interpretation of residual stress data are more simple and reliable using this thermo-mechanical analysis.
- The distortion prediction noticeably agrees with experimental measurements. The negligible variations are caused by the unclamping sequence during the experiment that was not incorporated in the simulation.

Acknowledgement

The financial support granted by the UGC-DAE-CSR Kalpakkam node, Government of India through the project no. CSR-KN/CRS-27/2011-12/639 entitled "Modeling of A-TIG welding of austenitic stainless steels and prediction of residual stresses" is greatly acknowledged. Also NIT, Trichy and IGCAR, Kalpakkam are acknowledged for the technical support.

References

1. Joy Varghese V M, Suresh M R and Siva Kumar D, Int. J. Adv. Man. Tech., (2012).

2. De A and DebRoy T, Sci. Tech. Wel. Jo., (2011), 16.
3. Eagar T W and Tsai N S, AWS Conv., (1983).
4. Tsai N S and Eagar T W, Mod. Cast. Weld. Pro., (1984).
5. Goldak J A, Chakravarti A and Bibby M, Meta. Tran. B, (1984), 15B.
6. Goldak J A, Oddy A, Gu M, Ma W, Mashaie A and Hughes E, IUTAM Symp., (1992).
7. Nguyen N T, Ohta A, Matsuoka K, Suzuki N and Maeda Y, Weld. Res. Sup., (1999).
8. Zhu X K and Chao Y J, Comp. Stru., (2002), 80.
9. Asserin O, Loredo A, Petelet M and Iooss B, Fini. Ele. Anal. Des., (2011), 47.
10. Barroso A, Canas J, Picon R, Paris F, Mendez C and Unanue I, Mat. Des (2010), 31.
11. Aarbogh H M, Hamide M, Fjaer H G, Mo A and Bellet M, J. Mat. Pro. Tech., (2010), 210.
12. Attarha M J and Far I S, J. Mat. Pro. Tech., (2011), 211.
13. M. Vasudevan, N. Chandrasekhar, V. Maduraimuthu, A.K. Bhaduri and Baldev Raj, Weld. in the World, (2011), 83.
14. P. Palanichamy, M. Vasudevan, and T. Jayakumar, Sci. and Tech. of Weld. and Join., (2009), 166.
15. 'Material properties for design', IGCAR data book, 1999.